The paper was published in the proceedings of the 10th International Conference on Scour and Erosion and was edited by John Rice, Xiaofeng Liu, Inthuorn Sasanakul, Martin McIlroy and Ming Xiao. The conference was originally scheduled to be held in Arlington, Virginia, USA, in November 2020, but due to the COVID-19 pandemic, it was held online from October 18th to October 21st 2021.

Numerical Simulation of Incipient Sediment Motion Driven by Fluid Flow

Tian-Xiong Zhao,[1,b] Xia Li,[2,a,b*]

[a] Key Laboratory of C&PC Structures, Ministry of Education, People's Republic of China;
[b] School of Civil Engineering, Southeast University, Nanjing 211189, People's Republic of China;
[1] zhaotianxiong@seu.edu.cn
[2] xia.li@seu.edu.cn
*Corresponding author.

ABSTRACT

Coupled CFD-DEM (Computational Fluid Dynamics-Discrete Element Method) simulation is applied to investigate the incipient sediment motion driven by fluid flow. In this method, the sediment particles are simulated through DEM, and fluid flow is simulated by CFD. The interaction between two phases is considered with an unresolved coupling method. In the calculation process, the CFD grid size is several times larger than the particle diameter, and the detailed flow around a single particle is not resolved. The process of a sediment erosion case involving 20000 spherical particles is studied numerically. The simulation result is then analyzed to study the pattern of sediment motion. In this study, drag force and buoyancy force are calculated to simulate the interaction between the two phases. A settling test of a spherical particle in still water is conducted as a benchmark case to assess the performance of the employed model. Simulation results succeed in describing the pattern of sediment motion.

INTRODUCTION

Sediment motion driven by fluid flow could be observed in many practical engineering problems, such as debris flow, failure of embankment dams and offshore structures. Existing research has provided a large amount of laboratory experimental data (Smart 1984; Rickenmann 1991; Camenen and Larson 2005; Loiseleux 2005; Lobkovsky et al. 2008; Zhou et al. 2015; Allen and Kudrolli 2017), and several empirical formulas proposed decades ago are still widely adopted in hydraulic engineering (Shields 1936; Meyer-Peter and Muller 1948; Einstein 1950; Bagnold 1973). However, considering the difficulty of observation, the experimental results could not provide trajectory and stress condition of an individual particle, which makes it difficult to study the mechanism of sediment motion and the interaction between fluid and particles.

Numerical simulation is another approach employed in existing research. The direct numerical simulation of the sediment motion driven by fluid flow could be conducted with two approaches, which respectively utilizes continuum model and discrete element model (DEM). Continuum model is established based on conservation of mass and momentum. Such approach could provide the velocity and concentration profile in the process of erosion (Pudasaini 2012; Domnik and Pudasaini, 2012; Domnik et al., 2013). However, continuum model lacks of micro scale description of particle motion (Zhao and Shan, 2013). To obtain such information, CFD-DEM coupled model is applied. Papista et al. (2011) have applied DNS-DEM model to analyse the initial stage of sediment motion. Zheng et al. (2018) implement a 2-D CFD-DEM simulation to simulate the erosion characteristics of the sediment bed in a micro and macro perspectives. The CFD-DEM model has been already proved to be reliable and efficient in many chemical engineering cases. However, it is relatively rare to apply 3-D CFD-DEM model to study erosion and scour.

In this study, a 3-D CFD-DEM model is established to simulate the erosion of 20000 particles by shear flow. The theoretical basis of applied model is firstly introduced. After that, the employed CFD-DEM model is applied to calculate the velocity of a single particle settling in still water. Comparison of simulation results and analytical solution could prove the capacity of the applied model to predict the interaction forces between particles and fluid. In the end, the observed sediment motion pattern is discussed.

METHODOLOGY

The CFD-DEM model consists of CFD and DEM modules. The open-source LAMMPS-based DEM code LIGGGHTS and CFD package OpenFOAM are employed in this study. The coupling framework is built based on the CFDEM project (Goniva et al. 2010). The coupling of particles and fluid is considered by the exchange of the information between two computing modules. The governing equations of particles are based on the Newton's second law and Hertz contact theory. Fluid is assumed to be continuous in this study, which could be numerically analyzed by solving locally averaged Navier-Stokes equations (Anderson and Jackson 1967).

The translational and rotational motions of an individual particle is treated following the equations shown below in LIGGGHTS (Kloss et al. 2012; Zhao and Shan 2013):

$$m_i \frac{dU_i^p}{dt} = \sum_{j=1}^{n_i^c} F_{ij}^c + F_i^f + F_i^g \quad (1)$$

$$I_i \frac{d\omega_i}{dt} = \sum_{j=1}^{n_i^c} M_i^j \quad (2)$$

where m_i and I_i denote the mass and moment of inertia of particle i. U_i^p and ω_i are the translational and rotational angular velocities. F_i and M_i are forces and torque acting on particle i. F^f denotes the interaction forces, which including buoyancy force and drag force in this study. F^c denotes contact forces between two particles. F^g denotes the force of gravity acting on particle i. In LIGGGHTS, the calculation of contact force between two particles is based on the Hertz contact law and Coulomb's friction criteria. The equations shown below are calculated by the CFD solver:

$$\frac{\partial(\varepsilon\rho)}{\partial t} + \nabla \cdot (\varepsilon\rho U^f) = 0 \quad (3)$$

$$\frac{\partial(\varepsilon\rho U^f)}{\partial t} + \nabla \cdot (\varepsilon\rho U^f U^f) - \varepsilon\nabla \cdot (\mu\rho U^f) = -\nabla \mathrm{p} - \mathrm{f}^{\mathrm{p}} + \varepsilon\rho g \quad (4)$$

To simulate the flow in this process, equation (3) and (4) are solved by CFD module, where U^f denotes the average velocity in a CFD cell. In this study, the icoFoam solver is modified in the OpenFOAM to solve the continuity equation. ε denotes the volume fraction of fluid in a cell. ρ is the averaged density calculated by the density of fluid and particle and their volume fraction. P is the fluid pressure. f^p denotes the interaction forces applied on fluid by particles.

The key to accurately simulate the sediment-water movement is the reasonable consideration of interaction forces between two phases. In this study, drag force and buoyancy force are considered. The drag forces is calculated by the equation used by Di Felice (1994):

$$F^d = \frac{1}{8} C_d \rho\pi d_p^2 (U^f - U^p) \left| U^f - U^p \right| \varepsilon^{1-\chi} \quad (5)$$

where C_d denotes the particle-fluid drag coefficient, ε^{χ} is applied to consider the influence of other particles in the system. Both C_d and χ could be calculated by Renolds number. According to previous research, Di Felice equation works well under low Renolds numbers condition (Kafui et al., 2002; Zhao and Shan, 2013). The buoyancy force of a spherical particle is calculated following the equation shown below:

$$F^{\mathrm{b}} = \frac{1}{6} \pi\rho d_p^3 g \quad (6)$$

In this study, the CFD time step is 10 times longer than the DEM time step. The CFD and DEM modules couple in each coupling interval. This approach has been proved to be promising by previous research (Zhao, 2013).

BENCHMARK CASE

A settling test of a spherical particle in still water is conducted as a benchmark case. A spherical particle with a diameter 0.1 mm and density of 3000 kg/m^3 is released from rest in a fluid container with a size of $0.05\text{m} \times 0.05\text{m} \times 0.1\text{m}$. The position and velocity of settling particle could be calculated analytically. To investigate the effect of the CFD mesh size on the accuracy of prediction, three different mesh sizes have been tested. The velocities of settling particles with different mesh sizes are shown in Figure 1.

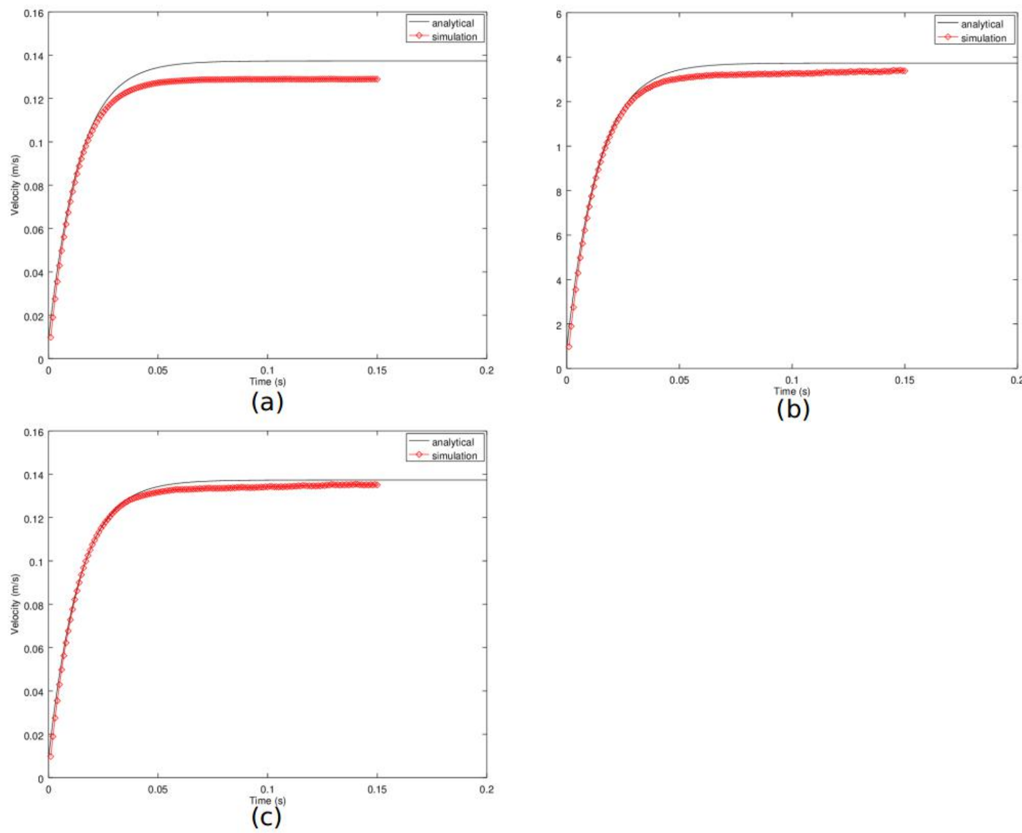

Figure 1. Comparison between simulation results with different mesh sizes. The ratio of mesh size to particle diameter in each figure is (a) 25:1, (b) 5:1, (c) 2.5:1

In Figure 1, (a), (b), (c) respectively represents the simulation results with a mesh size equals to 2.5 mm, 0.5 mm and 0.25 mm. Obtained simulation results are compared with analytical solution through Stokes equation. The errors and calculation time with different mesh sizes are shown in Table 1.

Table 1. Error and calculation time with different mesh sizes

Grid Size (mm)	CFD cells number	Error of the particle final velocity	Computing time (s)
2.5	320	6.093%	1
0.5	40000	2.557%	28
0.25	320000	1.614%	514

As the error dropped from 2.557% to 1.614%, the computing time increased about 20 times. Therefore, it is reasonable to claim that both error and calculation time are acceptable when the ration of CFD mesh size to the particle diameter is around 5:1. This became the basis for choosing the mesh size in our subsequent simulation.

APPLICATION TO SEDIMENT MOTION

The model is then applied to the investigation of sediment motion driven by shear flow. As shown in Figure.2, particles are placed in a container with periodical boundary, so that the departing particles return to the calculation region from the opposite side with the same velocity. With a laminar condition, the velocity of flow is distributed linearly from the top to the fluid-particle interface. Starting at a low velocity, the top velocity is gradually increased until the particles are observed to start moving. The detailed simulated condition could be found in Table 2.

Table 2. Simulation condition

Parameters	Value
Particle number	20000
Density of particles (kg/m3)	3000
Diameter of particles (m)	0.001
CFD time step (s)	1e-4
DEM time step (s)	1e-5
Coupling interval	10
Fluid density (kg/m^3)	1000
Dynamic viscosity of fluid	1e-6

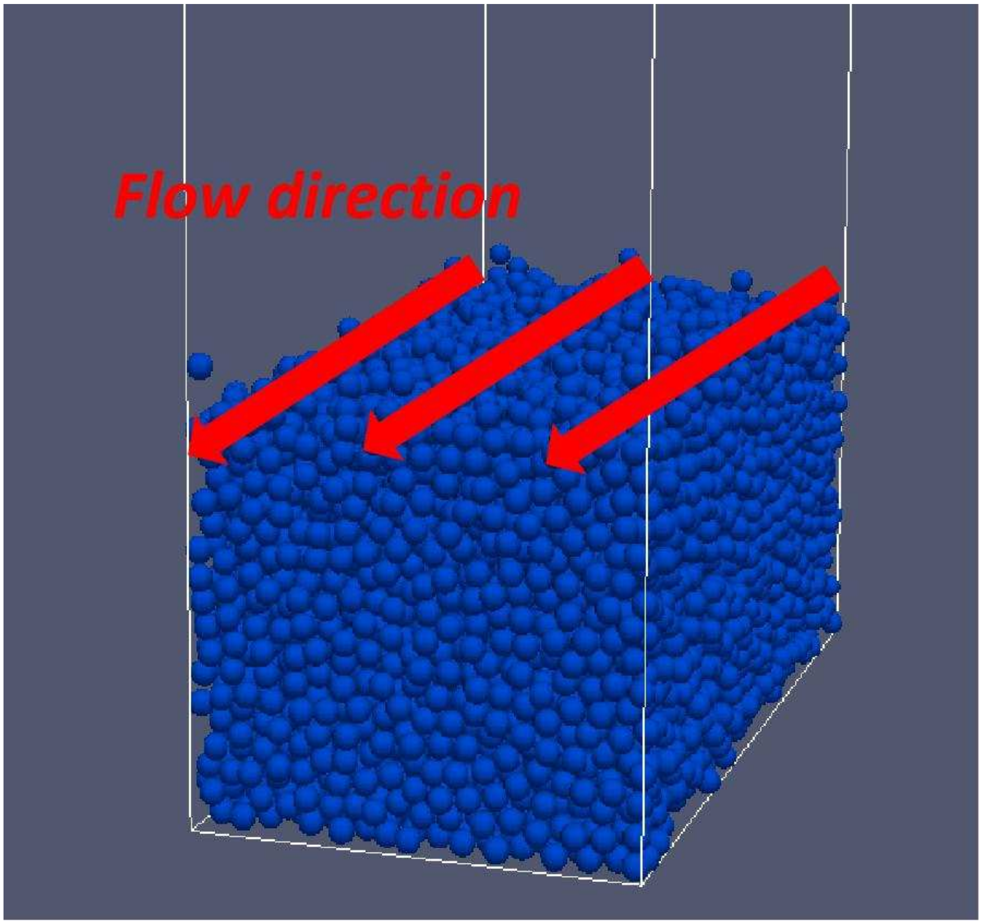

Figure 2. Simulation model and flow direction

In the initial stage, the flow is driven by the no-slip boundary at the top to form a linear velocity distribution. In this case, when the Shields number reaches 0.2, the particles are observed to start moving (Figure 3.a). Under the action of the shear stress caused by the shear flow, a part of particles at the top layer leap, suspend and crash the bed (Figure.3. b. c. d). As the moving particles are transported through the direction of the current, the morphology of sediment surface also changed. As a result of changed flow pattern near the fluid-sediment interface, the shear stresses are no longer large enough to move particles. The number of moving particles decreases over time as a self-organized steady state of the bed sediment is formed (Figure.3. e).

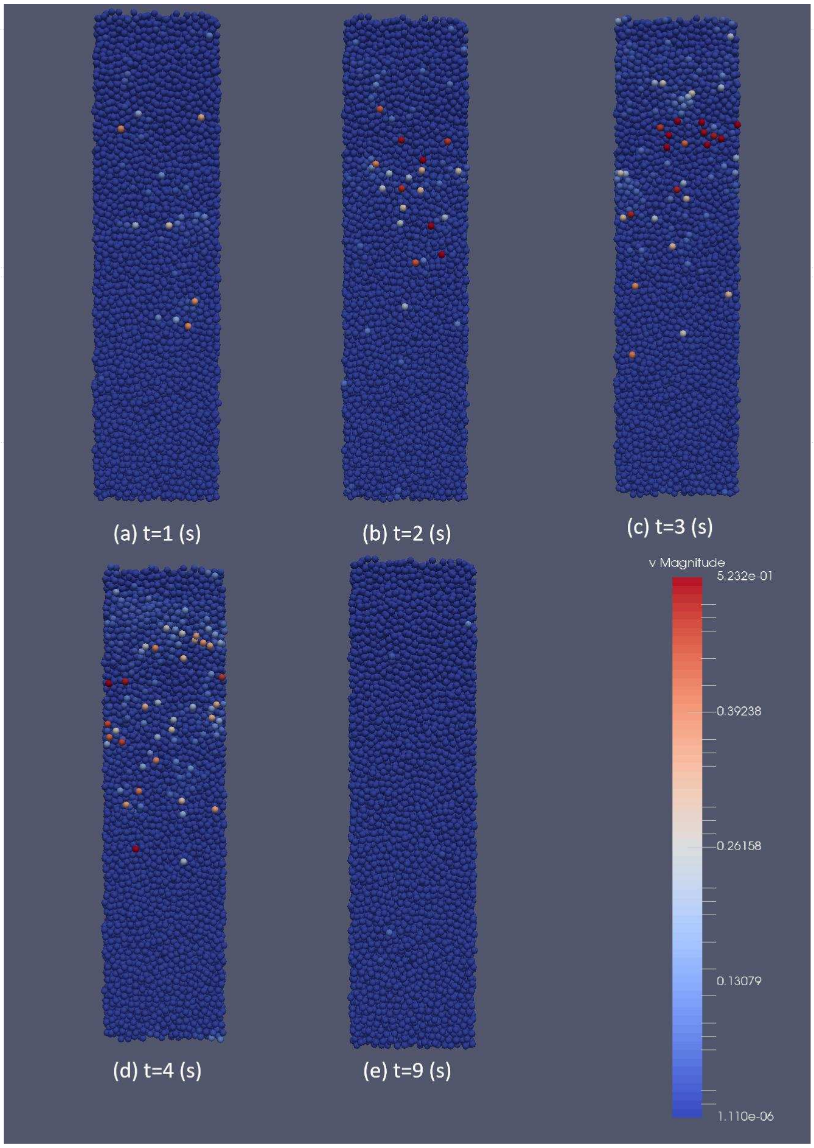

Figure 3. Velocity profile of particles at different times

CONCLUSION

(1) Settling of a particle in still water was simulated using an unresolved CFD-DEM approach. The performance of the employed CFD-DEM model has been assessed by comparing the simulation result and analytical solution of mentioned benchmark case. At an appropriate mesh size, the simulation result agrees well with the analytical solution.

(2) By applying the CFD-DEM model to the simulation of sediment transport driven by shear flow, detailed information of particles and flow could be obtained. The redistribution of particles near the sediment-fluid interface driven by shear stress was captured and recorded.
(3) Starting at a low velocity, the flow velocity is gradually increased until the particles start moving. Driven by the flow with a critical shear velocity, the particle velocity varies with time. At the initial stage, the particles moved as a result of the shear flow. Then the random redistribution of particles formed an uneven shape of the sediment bed. The hydrodynamics have adjusted in tandem with the bed so the shear stresses are no longer large enough to move particles. It is possible that the uneven bed height also impedes the further particle transport. The mechanism of the self-reorganization phenomenon may need further study. The comparison of the simulation results with the existing experimental results is in progress.

REFERENCES

Allen, Benjamin, and Arshad Kudrolli. "Depth resolved granular transport driven by shearing fluid flow." *Physical Review Fluids* 2.2 (2017): 024304.

Anderson, T. Bo, and Roy Jackson. "Fluid mechanical description of fluidized beds. Equations of motion." *Industrial & Engineering Chemistry Fundamentals* 6.4 (1967): 527-539.

Bagnold, Ralph Alger. "The nature of saltation and of 'bed-load'transport in water." *Proceedings of the Royal Society of London. A. Mathematical and Physical Sciences* 332.1591 (1973): 473-504.

Camenen, B., & Larson, M. (2005). "A general formula for non-cohesive bed load sediment transport." *Estuarine, Coastal and Shelf Science*, 63(1-2), 249-260.

Di Felice, R. (1994). "The voidage function for fluid-particle interaction systems." *International journal of multiphase flow*, 20(1), 153-159.

Domnik, B., & Pudasaini, S. P. (2012). "Full two-dimensional rapid chute flows of simple viscoplastic granular materials with a pressure-dependent dynamic slip-velocity and their numerical simulations." *Journal of Non-Newtonian Fluid Mechanics*, 173, 72-86.

Domnik, B., Pudasaini, S. P., Katzenbach, R., & Miller, S. A. (2013). "Coupling of full two-dimensional and depth-averaged models for granular flows." *Journal of Non-Newtonian Fluid Mechanics*, 201, 56-68.

Einstein, H. A.(1950). "The bed-load function for sediment transportation in open channel flows." *No. 1026. US Government Printing Office*.

Goniva, C., Kloss, C., Hager, A., & Pirker, S. (2010, June). "An open source CFD-DEM perspective." *In Proceedings of OpenFOAM Workshop, Göteborg* (pp. 22-24).

Kafui, K. D., Thornton, C., & Adams, M. J. (2002). "Discrete particle-continuum fluid modelling of gas–solid fluidised beds." *Chemical Engineering Science*, 57(13), 2395-2410.

Kloss, C., Goniva, C., Hager, A., Amberger, S., & Pirker, S. (2012). "Models, algorithms and validation for opensource DEM and CFD–DEM." *Progress in Computational Fluid Dynamics, an International Journal*, 12(2-3), 140-152.

Loiseleux, Thomas, et al. "Onset of erosion and avalanche for an inclined granular bed sheared by a continuous laminar flow." *Physics of fluids* 17.10 (2005): 103304.

Papista, E., Dimitrakis, D., & Yiantsios, S. G. (2011). "Direct numerical simulation of incipient sediment motion and hydraulic conveying." *Industrial & Engineering Chemistry Research*, 50(2), 630-638.

Pudasaini, S. P. (2012). "A general two - phase debris flow model." *Journal of Geophysical Research: Earth Surface*, 117(F3).

Rickenmann, D. (1991). "Hyperconcentrated flow and sediment transport at steep slopes." *Journal of hydraulic engineering*, 117(11), 1419-1439.

Shirole, A. M., & Holt, R. C. (1991). "Planning for a comprehensive bridge safety assurance program." *Transportation Research Record*, 1290, 39-50.

Smart, G. M. (1984). "Sediment transport formula for steep channels." *Journal of Hydraulic Engineering*, 110(3), 267-276.

Zhao, J., & Shan, T. (2013). "Coupled CFD–DEM simulation of fluid–particle interaction in geomechanics." *Powder technology*, 239, 248-258.

Zheng, H. C., Shi, Z. M., Peng, M., & Yu, S. B. (2018). "Coupled CFD-DEM model for the direct numerical simulation of sediment bed erosion by viscous shear flow." *Engineering geology*, 245, 309-321.

Zhou, Gordon GD, et al. "Experimental study on the triggering mechanisms and kinematic properties of large debris flows in Wenjia Gully." *Engineering Geology* 194 (2015): 52-61.